Selected papers presented at the 15th Symposium of Magnetic Measurements and Modelling SMMM'2025

Measurements and Analysis of Amorphous Ribbon Properties Under Non-Standard Operating Conditions

D. Stachowiak[a] and M. Najgebauer[b,*]

[a] *Poznan University of Technology, Faculty of Control, Robotics and Electrical Engineering, Piotrowo 3A, 61-138 Poznań, Poland*
[b] *Czestochowa University of Technology, Faculty of Electrical Engineering, al. Armii Krajowej 17, 42-200 Częstochowa, Poland*

Doi: 10.12693/APhysPolA.149.S120 *e-mail: mariusz.najgebauer@pcz.pl

The paper presents measurements and analysis of the magnetic properties of VITROVAC 6030 amorphous ribbons. Hysteresis loops were measured at a frequency of 1 kHz for standardized (sinusoidal) excitations and non-standard operating conditions, i.e., under harmonic flux density waveforms and in the presence of tensile stress. The effect of such operating conditions on the magnetic parameters was analysed.

topics: amorphous ribbons, harmonic excitations, tensile stress, hysteresis loop

1. Introduction

Amorphous ribbons are materials that exhibit extremely soft magnetic properties, including very low coercivity values and significantly reduced energy losses compared to conventional electrical steel sheets. However, these materials are characterized by both a lower saturation induction value and a higher magnetostriction coefficient [1–4].

Amorphous ribbons are produced by rapid solidification technology, in which a liquid metal alloy is transformed from the liquid phase to the solid phase without crystallization, as depicted in Fig. 1. The dimensions of the final amorphous ribbons are 0.02–0.04 mm in thickness and 140–215 mm in width. The magnetic properties of amorphous ribbons strongly depend on their chemical composition, especially on the dominant metallic elements, as shown in Table I [1–6].

Fe-based amorphous ribbons are mainly used as core material in energy-efficient distribution transformers operating at mains frequencies [3, 4, 7, 8]. Co-based ribbons, which, in addition to their soft magnetic properties, are characterized by mechanical hardness and a high elastic limit, are an ideal solution for applications such as electronic article surveillance, flexible antennae, magnetic sensors, as well as for high-frequency devices, including switched-mode power supplies, magnetic shielding, and wireless charging [3, 6, 9–11].

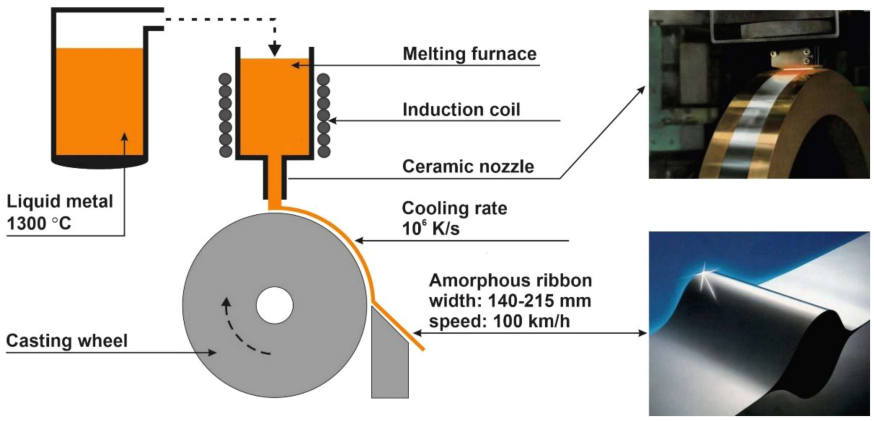

Fig. 1. Magnetic amorphous ribbons — technology production [4].

TABLE I

Chosen magnetic properties of amorphous ribbons [1–6]. Here, $P_{1.0/50}$ denotes the specific power loss measured at a magnetic flux density of 1.0 T and a frequency of 50 Hz.

Magnetic parameter	Fe-based amorphous ribbon[a] (thickness 0.03 mm)	Co-based amorphous ribbon[b] (thickness 0.03 mm)	Grain-oriented 3% SiFe steel (thickness 0.35 mm)
B_S [T]	1.30–1.56	0.40–1.00	1.90–2.03
H_C [A/m]	5–8	3	10–30
μ_i [–]	10×10^3	$50–100 \times 10^3$	10^3
$\mu_{\max}$ [–]	300×10^3	550×10^3	100×10^3
λ_S [–]	30×10^{-6}	$< 0.2 \times 10^{-6}$	-0.8×10^{-6}
$P_{1.0/50}$ [W/kg]	0.11	0.15	0.40

[a] $Fe_{78}Si_{13}B_9$ (Metglas 2605SA1), [b] $Co_{71,5}Fe_{2,5}Mn_2Mo_1Si_9B_{14}$ (VITROVAC)

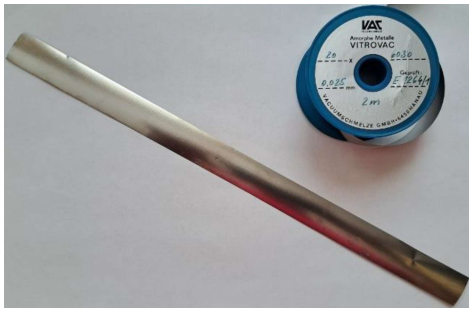

Fig. 2. The sample of Co-based amorphous ribbon (VITROVAC 6030).

Regardless of the type of magnetic materials and their application scope, magnetic circuits are designed based on manufacturers' catalog data (or measurements) obtained under standard excitations (i.e., a sinusoidal flux density waveform inside a magnetic sample), as defined in IEC 60404 standards [12–14]. However, magnetic cores in real electrical or electronic devices are usually exposed to non-standard operating conditions, such as harmonic or pulse-width modulated (PWM) excitation signals, as well as mechanical stresses, which can negatively affect their magnetic properties.

In the case of amorphous ribbons, the influence of non-standard operating conditions has been the subject of numerous studies [15–20]. Particular attention has been paid to the effects of non-sinusoidal excitation waveforms, such as harmonic-rich or pulse-width-modulated signals, which commonly occur in modern power-electronic systems. Under such excitation, additional minor hysteresis loops are formed and are superimposed on the major hysteresis loop, resulting in increased specific core losses compared to sinusoidal magnetization [16, 17]. This effect has been experimentally observed for amorphous ribbon cores and has been shown to intensify with increasing harmonic content.

Another important factor influencing the magnetic behavior of amorphous ribbons is mechanical stress. Due to the relatively high magnetostriction of Fe-based amorphous alloys, tensile and compressive stresses introduced during manufacturing processes or operation significantly affect the magnetization characteristics and loss mechanisms [15, 18]. Tensile stress applied along the magnetizing direction may reduce the required magnetizing field and decrease iron losses, whereas compressive stress generally leads to an increased magnetizing field strength and a pronounced loss deterioration [18, 19]. Even in the case of Co-based amorphous ribbons, which are characterized by near-zero saturation magnetostriction, residual stresses originating from lamination, bonding, or sample fixation can modify the magnetic anisotropy and dynamic magnetization processes, especially under non-standard excitation conditions [17, 20]. As a result, magnetic properties measured under standardized sinusoidal excitation may differ substantially from those observed under real operating conditions. This highlights the necessity of dedicated experimental investigations that consider both waveform distortion and stress effects. This article presents the measurement results and analyses the effects of harmonic flux density waveforms and applied tensile stress on the magnetic properties of cobalt-based amorphous ribbons.

2. Sample and measurements

In our tests, we examined a Co-based amorphous magnetic material, type VITROVAC 6030. This amorphous material has a saturation flux density of $B_S = 0.80–0.82$ T and vanishing saturation magnetostriction of $\lambda_S \approx 0$, according to the manufacturer's data [6, 9].

The magnetic properties of the Co-based sample were measured using the MPG-200 computer system by Brockhaus Measurements (Germany),

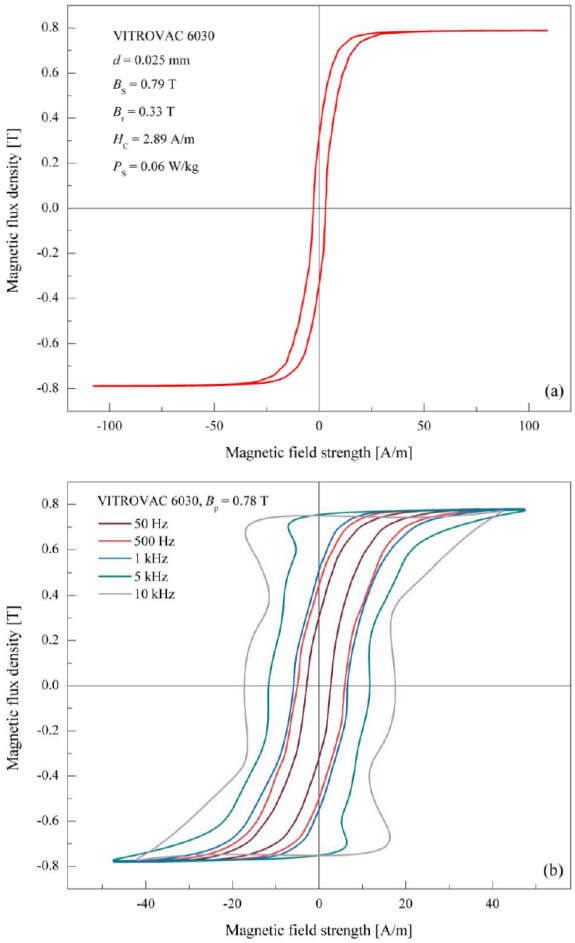

Fig. 3. Hysteresis loops for the VITROVAC 6030 ribbon: (a) saturation loop, (b) major loops measured at different excitation frequencies.

for standardized (sinusoidal) and non-standardized (harmonic) flux density waveforms inside the sample. The amorphous sample was a single ribbon (length 300 mm, width 25 mm, thickness 0.025 mm and weight 1.21 g), as depicted in Fig. 2. The sample was magnetized using a single-strip tester (SST) yoke with 200 turns of primary (magnetizing) and secondary (measuring) windings, which provided uniform magnetization of the sample.

2.1. Measurements for sinusoidal flux density waveforms

In the first stage, magnetic measurements were carried out for a sinusoidal flux density waveform with a frequency of 50 Hz in order to compare the measured magnetic properties with the manufacturer's data of tape-wound cores [6, 9]. The measured saturation hysteresis loop and the obtained values of magnetic parameters are depicted in Fig. 3a. The measured magnetic parameters are consistent with the manufacturer's data, e.g., the measured saturation flux density is $B_S = 0.79$ T compared to the catalogue value of 0.80–0.82 T. Figure 3b presents hysteresis loops measured for sinusoidal flux density waveforms of higher frequencies. For magnetizing frequencies up to 1 kHz, the shapes of the hysteresis loops are similar to the basic saturation loop (i.e., for 50 Hz), only their widening is observed, which is related to the increase in eddy current losses when the magnetization frequency increases. However, for magnetizing frequencies above 1 kHz, significant deformations of the hysteresis loop are observed in the area of the so-called "hysteresis knees". This phenomenon was not taken into account in the research presented in this paper, therefore further magnetic measurements were limited to the frequency of 1 kHz, representing the area of increased operating frequencies of electrical devices.

TABLE II

Specific energy loss (P_S) of the VITROVAC 6030 ribbon under harmonic excitations.

B waveform	P_S [W/kg]
sine	2.79
3rd harm. $(0.3, 45°)$	3.23
3rd harm. $(0.5, 45°)$	3.79
4th harm. $(0.3, 0°)$	4.04
4th harm. $(0.5, 0°)$	5.28

2.2. Measurements under harmonic flux density waveforms

As mentioned earlier, magnetic cores in electrical and electronic devices often operate with non-sinusoidal excitations. To evaluate the effect of such excitations on the magnetic properties of the VITROVAC 6030 ribbon, measurements were carried out for harmonic magnetic induction waveforms. The harmonic excitation was shaped by the measurement system according to the following relationship

$$B = B_1 \sin(\omega t) + \sum_n B_n \sin(n\omega t + \theta_n), \qquad (1)$$

where: B_1 — amplitude of the fundamental excitation component (i.e., for the magnetization frequency 1 kHz), B_n — amplitude of the n-th harmonic component, θ_n — phase angle of the n-th harmonic component [21].

Hysteresis loops measured for selected harmonic flux density waveforms with different amplitude ratios B_n/B_1 and phase angles θ_n are depicted in Figs. 4 and 5. The obtained results indicate that the harmonic waveforms of magnetic flux density are the source of additional minor hysteresis loops. The position of these minor loops relative to the

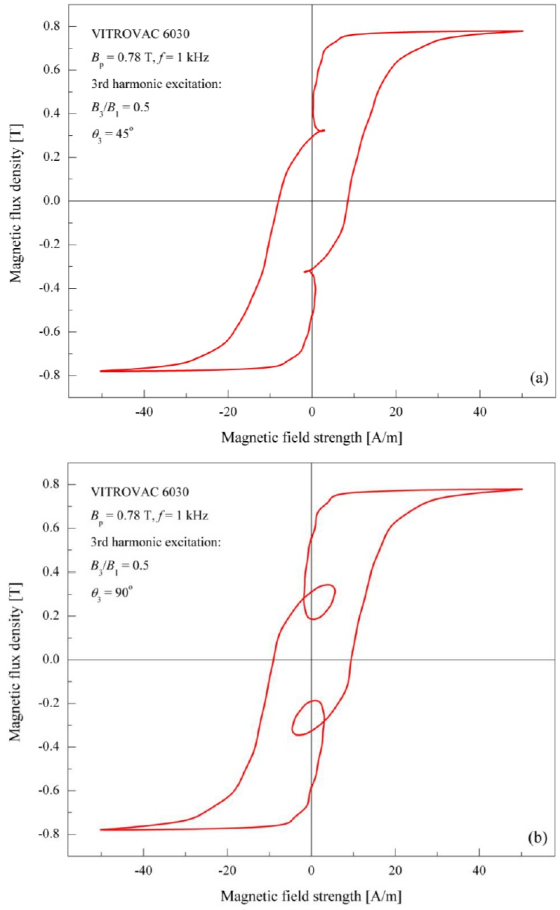

Fig. 4. Hysteresis loops for the VITROVAC 6030 ribbon measured under the 3rd harmonic flux density waveforms.

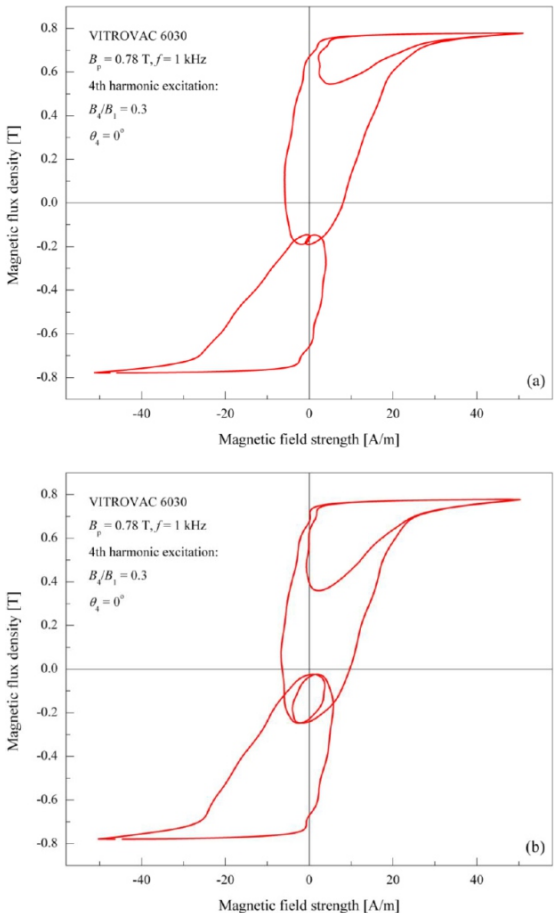

Fig. 5. Hysteresis loops for the VITROVAC 6030 ribbon measured under the 4th harmonic flux density waveforms.

major hysteresis loop is determined by the values of the phase angles, while their amplitudes by the values of the ratio B_n/B_1.

The occurrence of minor hysteresis loops — which, similarly to the major loop, represent additional energy dissipation processes in the sample — contributes to the increase in specific energy losses under harmonic magnetic flux density waveform excitations, as shown in Table II.

TABLE III

Magnetic properties of the VITROVAC 6030 ribbon under tensile stress (at a fixed value of B_p).

Tensile stress [MPa]	B_p [T]	$H_{\max}$ [A/m]	P_S [W/kg]
0	0.78	45.8	2.79
140		56.9	2.32
420		192.3	1.01
700		559.3	0.48

2.3. Measurements in the presence of tensile stress

Amorphous cores are manufactured as wound cores, consisting of many thin layers. The core forming process can generate internal stresses in the amorphous ribbons. Other technological operations during core production, such as cutting, winding, and final assembly, can be additional sources of internal stresses.

Measurements of the magnetic properties of the VITROVAC 6030 ribbon were carried out using the Brockhaus SST under stress system, connected to the MPG-200 measuring system. This yoke allows for the generation of both tensile and compressive stresses in the sample [22]. However, due to the mechanical properties of amorphous ribbons (low thickness and high brittleness), magnetic measurements were carried only under tensile stress. Figure 6a presents hysteresis loops measured in the presence of tensile stresses at a fixed value of magnetic flux density close to the saturation state. As the level of tensile stress applied to the sample increases, the measured hysteresis loops become narrower and more tilted. The applied tensile stresses

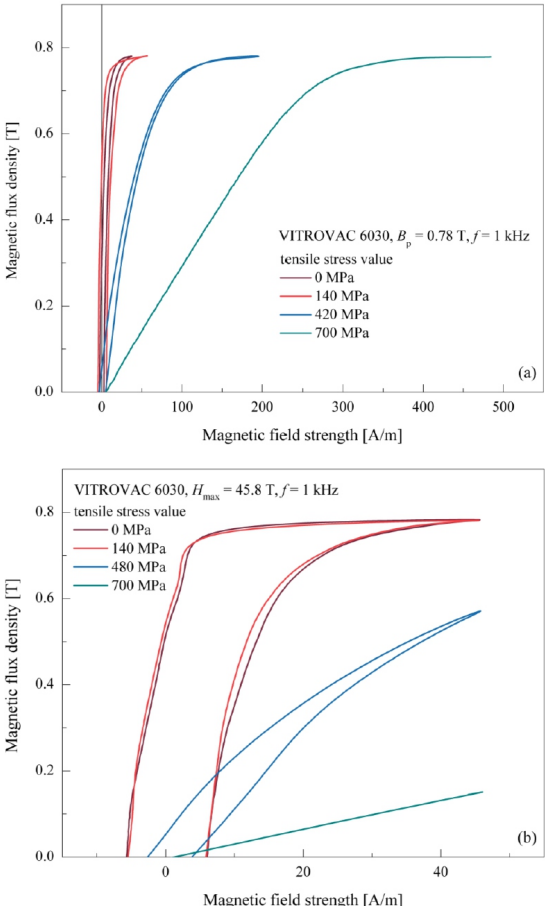

Fig. 6. Hysteresis loops for the VITROVAC 6030 ribbon measured under tensile stress: (a) at a fixed value of magnetic flux density B_p, (b) at a fixed value of magnetic field strength $H_{\max}$.

TABLE IV

Magnetic properties of the VITROVAC 6030 ribbon under tensile stress (at a fixed value of $H_{\max}$).

Tensile stress [MPa]	B_p [T]	$H_{\max}$ [A/m]	P_S [W/kg]
0	45.8	0.78	2.79
140		0.78	2.60
420		0.57	0.67
700		0.15	0.05

deform the domain structure inside the sample, which on the one hand reduces the level of specific energy loss, but at the same time significantly increases the value of the magnetic field strength for which the sample reaches a state close to saturation ($B_p = 0.78$ T), as presented in Table III. Figure 6b presents under-stress hysteresis loops measured at a fixed value of magnetic field strength. Similarly to the previous case, the occurrence of tensile stresses worsens the magnetic properties of the material (lower peak induction), but improves its functional properties (reduced specific energy loss), as presented in Table IV.

3. Conclusions

The magnetic properties of the VITROVAC 6030 amorphous ribbon were measured and analyzed under the influence of both harmonic excitations and tensile stresses, applied to the sample. In the case of harmonic flux density waveforms, the specific loss in the amorphous sample increased due to the presence of additional, minor hysteresis loops. However, the effect of tensile stresses on the magnetic properties of the amorphous ribbon was ambiguous, as they worsened important material parameters (e.g., saturation flux density) while simultaneously reducing the specific loss of the material.

The presented results confirm that the magnetic properties of the amorphous VITROVAC 6030 ribbon are strongly dependent on non-standard (i.e., other than those specified in IEC 60404 standards) operating conditions. These results indicate the need to determine the properties of magnetic materials under conditions that closely resemble the actual operating conditions of the magnetic core.

References

[1] M.E. McHenry, M.A. Willard, D.E. Laughlin, *Prog. Mater. Sci.* **44**, 291 (1999).

[2] R. Hasegawa, *Mater. Sci. Eng. A* **375**, 90 (2004).

[3] R. Hasegawa, *J. Magn. Magn. Mater.* **304**, 187 (2006).

[4] M. Najgebauer, in: *10th Int. Conf. on Electrical, Electronic and Computing Engineering (IcETRAN), East Sarajevo (Bosnia and Herzegovina)*, 2023, p. 1.

[5] Magnetic alloy 2605SA1 (iron-based), Metglas Inc., 2009.

[6] "Soft Magnetic Materials and Semi-Finished Products", Vacuumschmelze GmbH & Co. KG, Germany 2002.

[7] N. DeCristofaro, *MRS Bulletin* **23**, 50 (1998).

[8] R. Hasegawa, D. Azuma, *J. Magn. Magn. Mater.* **20**, 2451 (2008).

[9] "VITROPERM 500 F — VITROVAC 6030 F: Tape Wound Cores for Power Transformers in Switched Mode Power Supplies", Vacuumschmelze GmbH & Co. KG, Germany 2003.

[10] F. Mazaleyrat, in: *Handbook of Magnetism and Magnetic Materials*, Eds. J.M.D. Coey, S.S.P. Parkin, Springer International Publishing, 2021, p. 1435.

[11] W. Wang, J. Fan, C. Li, Y. Yu, A. Wang, S. Li, J. Liu, *Energies* **18**, 482 (2025).

[12] IEC 60404-2:1996: "Magnetic materials. Part 2: Methods of measurements of the magnetic properties of electrical steel sheet by means of an Epstein frame", International Electrotechnical Commission, Geneva (Switzerland) 1996.

[13] IEC 60404-3:2022: "Magnetic materials. Part 3: Methods of measurement of the magnetic properties of magnetic sheet and strip by means of a single sheet tester", International Electrotechnical Commission, Geneva (Switzerland) 2022.

[14] IEC 60404-6:2018: "Magnetic materials. Part 6: Methods of measurement of the magnetic properties of magnetically soft metallic and powder materials at frequencies in the range 20 Hz to 100 kHz by the use of ring specimens", International Electrotechnical Commission, Geneva (Switzerland) 2018.

[15] J. Xiao, L. Li, A. Cai, D. Ding, *IEEE Trans. Magn.* **61**, 1 (2025).

[16] J. Li, S. Yue, Y. Dou, J. Zhou, Y. Li, *AIP Adv.* **15**, 035119 (2025).

[17] Y. Guo, L. Liu, X. Ba, H. Lu, G. Lei, P. Sarker, J. Zhu, *Energies* **15**, 7798 (2022).

[18] T. Mizuta, Y. Tani, K. Fujiwara, *IEEE Trans. Magn.* **54**, 1 (2018).

[19] J. Egbu, A. Leary, K. Byerly, S. Simizu, E. Thiesen, P. Ohodnicki, *IEEE Trans. Magn.* **59**, 1 (2023).

[20] A. Masood, H.A. Baghbaderani, K.L. Alvarez, J.M. Blanco, Z. Pavlovic, V. Ström, P. Stamenov, C.O. Mathuna, P. McCloskey, *J. Magn. Magn. Mater.* **519**, 167469 (2021).

[21] M. Najgebauer, D. Gzieł, J. Kalinowski, B. Koprivica, *Energies* **17**, 5865 (2024).

[22] M. Gębara, M. Najgebauer, R. Gozdur, K. Kopiecki, K. Chwastek, *Appl. Sci.* **16**, 78 (2026).